$$\times \exp(J_{00} + J_{10}u + J_{01}s + J_{11}su + J_{20}u^2 + J_{02}s^2) , \quad (9)$$

where

$$\begin{aligned} J_{00} &= Z^2 Y^{*2}/(2|Y|^2 W) - [\mathrm{Re}(ZY^*)]^2/2|Y|^2, \\ J_{10} &= -2ZY^*/W, \quad J_{11} = 4iY^*/W, \\ J_{01} &= 2iZY^{*2}/(|Y|^2 W) + 2Q_{22}\,\mathrm{Re}(ZY^*)/|Y|^2 , \\ J_{20} &= 2/W - 1, \\ J_{02} &= 2Y^{*2}/(|Y|^2 W) - 2Q_{22}^2/|Y|^2 + 1, \\ W &= |Y|^2 + XY^*, \quad Y^* = Q_{12} - iQ_{22}. \end{aligned} \quad (10)$$

If both sides of $\partial I/\partial u = (J_{10} + J_{11}s + 2J_{20}u)I$ and $\partial I/\partial s = (J_{01} + J_{11}u + 2J_{02}s)I$ are expanded in Taylor series around $u = s = 0$ the following recurrence relations are obtained:

$$\begin{aligned} I_{m+1,n} &= J_{10} I_{m,n} + nJ_{11} I_{m,n-1} + 2mJ_{20} I_{m-1,n} , \\ I_{m,n+1} &= J_{01} I_{m,n} + mJ_{11} I_{m-1,n} + 2nJ_{02} I_{m,n-1} . \end{aligned} \quad (11)$$

All the integrals $I_{m,n}$ can be easily calculated from Eqs. (11) in terms of $I_{0,0} = (\mathrm{Re}\, a)^{1/4}[2\pi/(1+a)]^{1/2} \exp J_{00}$. Finally, the transition probability from the initial state n to the final state m reads

$$P_{mn} = \lim_{\substack{t\to\infty \\ t_0\to-\infty}} |I_{m,n}|^2/(2^{m+n}\pi m!n!). \quad (12)$$

It is worth noting that Eqs. (9)–(12) in this note are equivalent to Eqs. (2.55)–(2.60) in Ref. 2.

Since the present method is much simpler than others used before[2,5] it may facilitate the calculation of transition probabilities when there is more than one degree of freedom. In this case it is necessary to make use of first- and second-order differential equations for F involving linear and bilinear terms in coordinate and momenta.

One can also proceed in a different way. Let F be the generating function for the set of eigenfunctions of H_0 which, in general, will describe a set of M uncoupled harmonic oscillators. Clearly, F will be an eigenfunction of $H_F = T + (E - TF/F)$ with eigenvalue E, where T is the kinetic energy operator in H_0. Therefore, the form of $F_t = UF$ is obtained from the fact that it is an eigenfunction of $(H_F)_t = UH_F U^+$, which is obviously a quadratic Hamiltonian because F is a product of Gaussian functions.

[1] J. D. Keller, J. Chem. Phys. **56**, 6108 (1972); G. D. Billing, Chem. Phys. **33**, 227 (1978).
[2] B. Gazdy and D. A. Micha, J. Chem. Phys. **82**, 4926 (1985).
[3] J. Recamier, D. A. Micha, and B. Gazdy, Chem. Phys. Lett. **119**, 383 (1985); J. Chem. Phys. **85**, 5093 (1986).
[4] F. M. Fernández and E. A. Castro, Phys. Lett. A (in press).
[5] L. F. Landovitz, A. M. Levine, E. Ozizmir, and W. M. Schreiber, J. Chem. Phys. **78**, 291 (1983).

Antiresonance in autoionizing Rydberg series of naphthalene

Jack A. Syage[a] and John E. Wessel[b]
The Aerospace Corporation, P. O. Box 92957, Los Angeles, California 90009

(Received 2 June 1987; accepted 3 August 1987)

We report clear evidence of asymmetric Fano line profiles observed in autoionizing Rydberg series of jet-cooled naphthalene. These unusual line shapes, referred to as antiresonances, occur by degenerate resonance interference of a discrete state with a continuum when both carry oscillator strength from a common initial or intermediate state.[1,2] The line profiles are extremely informative, providing a measure of bound–continuum coupling interactions and oscillator strengths involving discrete and continuum states.

Recently, extensive autoionization Rydberg series above the lowest ionization limits were reported for benzene,[3,4] aniline,[5] *trans*-stilbene,[6] pyrazine,[7] DABCO,[8] and ABCO.[9] In each case, the autoionization spectra consisted of relatively sharp and symmetric transitions superimposed on an otherwise continuous background. Recently, Goto, Fujii, and Ito[7] suggested that some features in pyrazine autoionization spectra can be explained in terms of the Fano model. The only other evidence for Fano-type effects in polyatomic spectra consists of unassignable features in single photon Rydberg transitions below the adiabatic ionization potential.[10] To our knowledge, the present results represent the first clear and informative example of asymmetric Fano line profiles for a large molecule. However, good examples of antiresonance exist for diatomic molecules.[1,11]

Our pulsed supersonic molecular beam apparatus and time-of-flight (TOF) mass spectrometer have been described in detail elsewhere.[12] Briefly, the output of two independently tunable dye lasers are frequency doubled to generate ω_1 and ω_2. Naphthalene was introduced into a differentially pumped molecular beam apparatus via a pulsed supersonic nozzle heated to 70 °C and under 40 psi He. Two-photon ionization signals arising from one-color excitation by the laser scanning ω_2 were suppressed by operating a shutter that blocked the ω_1 pulse on alternate triggers. The ω_2 only signal was then subtracted from the $\omega_1 + \omega_2$ signal, providing the signal-to-noise ratio required to resolve the weak Rydberg series superimposed on the continua.

A vibrationally selected autoionizing excitation spectrum is presented in Fig. 1 for a region above the adiabatic

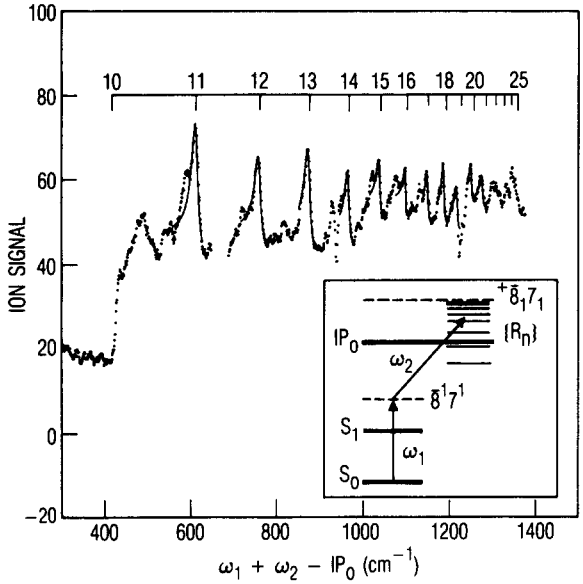

FIG. 1. Double resonance autoionization spectrum of naphthalene recorded via the intermediate state $S_1(\bar{8}^1 7^1)$ (see excitation scheme, insert). The energy scale is relative to the vertical ionization potential at 65 665 cm^{-1}. The $^+\bar{8}_1$ ionization threshold at 420 cm^{-1} was red shifted by applying a 150 V/cm electric field during the scan of the 300–650 cm^{-1} region. The dips at 950 and 1230 cm^{-1} are residual effects of the subtraction method used to remove the ω_2 only ionization signal.

ionization level IP_0. Excitation by ω_1 to the $\bar{8}^1 7^1$ nontotally symmetric combination vibration of S_1 followed by ω_2 excitation reveals a strong Rydberg series, R_n, converging to the presumed $^+\bar{8}^1 7^1$ ionization threshold at 1537 cm^{-1} (vs 1422 cm^{-1} in S_1). Additional structure is evident in Fig. 1, which appears to be part of other Rydberg series. (An attempt was made to expose lower energy Rydberg states by applying a 150 V/cm electric field to red shift the underlying continuum so as to overlap with other states. No new transitions, however, were observed.) The prominence of the R_n $(\bar{8}^1 7^1)$ series by ω_2 excitation is indicative of a propensity for $\Delta v = 0$ transitions. Excitation of the totally symmetric 7^1 vibration of S_1 (at 988 cm^{-1}) by ω_1 followed by ω_2 excitation gave a similar Rydberg series for 7^1. Other transitions were studied that did not include ν_7 in S_1, however, no Rydberg autoionization was observed.

Although several theories of antiresonance line shapes have been published[13] which extend the original treatment by Fano,[2] these theories, for the most part, consider absorption below ionization energies where the resonantly interacting diffuse states are not smooth continua. The involvement of a smooth ionization continuum in the present case allows us to use a simple formulation[1,11] of Fano's original theory for the line shape $L(\epsilon)$:

$$L(\epsilon) = \frac{(q+\epsilon)^2}{(1+\epsilon^2)},$$

where $\epsilon = 2\hbar(\omega - \omega_0)/\Gamma$, ω, and ω_0 are the excitation and line center frequency, respectively, Γ is the spectral linewidth, and q is the line profile index and is proportional to the ratio of transition moments to the discrete and continuum states. Calculated Fano line profiles are superimposed

TABLE I. Fano profile analysis for autoionizing Rydberg series in naphthalene.

n	Line center[a] (cm^{-1}) Obs.[b]	Calc.[c]	Linewidth (cm^{-1})	Lifetime (ps)	q
10		417.6			
11	615	613.6	18	0.30	−3.5
12	762	762.3	17	0.31	−3.0
13	877.5	877.7	17	0.31	−2.8
14	969.5	969.2	12	0.44	−2.5
15	1042	1042.8	10	0.53	−2.0
16	1102.5	1103.0	6	0.89	−1.5
17	1153	1152.9	8	0.67	−2.4
18	1191	1194.6	7	0.76	−2.2
19	1222	1229.9	8	0.67	−2.0
20	1255	1260.0	7	0.76	−2.2
21	1280.5	1285.8	9	0.59	−2.5
22		1308.3			

[a] Reported relative to $IP_0 = 65\,665$ cm^{-3} (Ref. 1).
[b] Determined from Fano profile best fit analysis.
[c] Rydberg series calculated for $IP(^+\bar{8}_1 7_1) - IP_0 = 1537$ cm^{-1} and $\delta = 0.10$.

onto the observed data in Fig. 1 and the best fit values reported in Table I. Of particulr interest is the narrowness of the lines and consequently the rather long-lived nature of these states relative to the few reported lifetimes for aromatic autoionization states. (Compare to upper limits of 50 fs for aniline[5] and 5 fs for benzene[3]). Even longer lifetimes are indicated for naphthalene-d_8 on the basis of preliminary work,[14] showing linewidths approaching the rotational bandwidth of about 3 cm^{-1} achieved under the present expansion conditions. This is indicative of small vibrational–electronic coupling between the Rydberg states and the ion. Within experimental error, the linewidths are proportional to n^{-3}, as predicted by theory.[15]

The autoionizing features in Fig. 1 were fitted to the $n = 11$ to 21 members of a Rydberg series that converges to $IP_0 + 1537$ cm^{-1} and has a quantum defect of $\delta = 0.10$. The calculated line frequencies are in good agreement with the observed values obtained from the Fano line profile analysis (Table I), even though we have held δ, constant over the entire region of interest. The low value of δ is consistent with a d series,[1] which in turn, is consistent with the large transition moment from the $S_1(\pi, \pi^*)$ intermediate state if we consider a qualitative $\Delta l = 1$ selection rule. Using the derived Rydberg values, the first member of the observed series $3d$ is calculated to occur at about 13 045 cm^{-1} below IP_0, which is consistent with term values for d series in benzene.[4]

The authors gratefully acknowledge the valuable assistance of Mr. Larry Pruitt in conducting these experiments. This work was supported by the Department of Energy, Office of Health and Environment, under Contract No. DE-FG03-86ER6039.

[a] Aerosphysics Laboratory.
[b] Chemistry and Physics Laboratory.

[1] (a) M. B. Robin, *Higher Excited States of Polyatomic Molecules* (Academic, New York, 1974), Vol. I; (b) J. Berkowitz, *Photoabsorption, Photoionization, and Photoelectron Spectroscopy* (Academic, New York, 1979).

[2]U. Fano, Phys. Rev. **124**, 1866 (1961); U. Fano and J. W. Cooper, Rev. Mod. Phys. **40**, 441 (1968).
[3](a) M. A. Duncan, T. G. Dietz, and R. E. Smalley, J. Chem. Phys. **75**, 2118 (1981); (b) M. Fujii, T. Kakinuma, N. Mikami, and M. Ito, Chem. Phys. Lett. **127**, 297 (1986).
2
[4](a) R. L. Whetten, S. G. Grubb, C. E. Otis, A. C. Albrecht, and E. R. Grant, J. Chem. Phys. **82**, 1115 (1985); (b) S. G. Grubb, C. E. Otis, R. L. Whetten, E. R. Grant, and A. C. Albrecht, *ibid*, **82**, 1135 (1985).
[5](a) J. Hager, M. A. Smith, and S. C. Wallace, J. Chem. Phys. **84**, 6771 (1986); (b) **83**, 4820 (1985).
[6]T. Suzuki, N. Mikami, and M. Ito, Chem. Phys. Lett. **120**, 333 (1985).
[7]A. Goto, M. Fujii, and M. Ito, J. Phys. Chem. **91**, 2268 (1987).
[8]M.Fujii, T. Ebata, N. Mikami, and M. Ito, J. Phys. Chem. **88**, 4265 (1984).
[9]M. Fujii, N. Mikami, and M. Ito, Chem. Phys. **99**, 193 (1985).
[10]R. Scheps, D. Florida, and S. A. Rice , J. Chem. Phys. **56**, 295 (1972).
[11]A. H. Kung, R. H. Page, R. J. Larkin, Y. R. Shen, and Y. T. Lee, Phys. Rev. Lett. **56**, 328 (1986).
[12](a) J. A. Syage and J. E. Wessel, J. Chem. Phys. **87**, 3313 (1987); (b) Appl. Opt. (to be published).
[13](a) S. D. Druger, J. Chem. Phys. **67**, 3238 (1977); (b) D. Florida, R. Scheps, and S. A. Rice, Chem. Phys. Lett. **15**, 490 (1972).
[14]To be published.
[15]R. S. Berry, J. Chem. Phys. **45**, 1228 (1966); J. N. Bardsley, Chem. Phys. Lett. **1**, 229 (1967); S. E. Neilsen and R. S. Berry, *ibid.* **2**, 503 (1968).

COMMENTS

Response to the paper: "Conformation kinetics of methyl nitrite. IV"

S. H. Bauer
Department of Chemistry, Baker Laboratory, Cornell University, Ithaca, New York 14853-1301

(Received 16 June 1986; accepted 16 July 1987)

Our measurements of relaxation times for the syn–anti isomerization of CH_3ONO[1] have been criticized by True *et al.*[2] They claim that our conclusions were based on faulty data. Their statements that we derived our rate constants entirely from runs at the coalescence condition, misapplied the expression $k_{coal} = \pi\Delta\nu/\sqrt{2}$, and neglected to correct for population changes with temperature are false. Reference to our paper shows that we used *both* line shape analysis and coalescence data, and allowed for temperature changes. It is my contention that their more extensive sets of data, while they differ from our early measurements by about a factor of 2, are in complete agreement with our initial observation relative to the crucial feature, that the experimentally derived bimolecular rate constants *increase with declining pressures* for $p < 20$ (or 40) Torr, contrary to conventional RRKM predictions.

Our disagreement concerns the *interpretation* of these data with respect to the magnitude of IVR times in CH_3ONO. Therefore, I propose that four sets of unimolecular rate constants published by True and co-workers[1,3] be reanalyzed. Their published k_{uni}'s were converted to k_{bi}^{exp} and *ratios* plotted in Fig. 1, so that different temperature runs were reduced to a common scale. For each set, the bimolecular rate constants were divided by the corresponding rate constant listed in their tables either for 40 Torr (upper scale) or 17 Torr (the maximum value listed; lower scale). Irrespective of what error limits they assigned, or whether all the runs were made under optimum conditions, it is obvious that their k_{bi}^{exp} *are not constant*; there is a general, *uniform* increase with decreasing pressure; the upward trend, upon which small random experimental fluctuations are superposed, is consistent. The deviations from unity start at 40 or 17 Torr. A similar trend also appeared in our data, indicating that the deviations follow an $[M]^{-1}$ dependence, as can be readily verified:

$$k_{bi}^{exp} = k_{bi}^{lim} + \frac{\alpha}{1+\beta[M]}$$
$$\Rightarrow k_{bi}^{lim} + \theta/[M], \quad \text{when } \beta[M] \gg 1. \qquad (1)$$

This behavior is typical of cyclohexane, tetrahydropyrane, and SF_4, except that the departures for these are even more

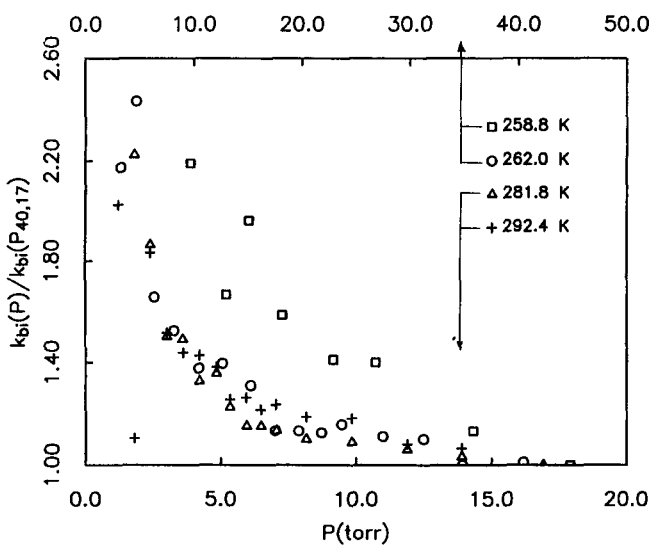

FIG. 1. Relative magnitudes of experimental bimolecular rate constants, plotted vs sample pressures. Read top scale for 259 and 260 K, and the bottom scale for 282 and 292 K.

